Emittance Bounds for Transient Radiative Cooling of a Scattering Rectangular Region

Robert Siegel*
NASA Lewis Research Center, Cleveland, Ohio

Transient cooling was analyzed for a two-dimensional gray rectangular region that emits, absorbs, and isotropically scatters radiation. The region, initially at uniform temperature, is placed in surroundings at a much lower temperature. The cooling analysis yields two simultaneous equations for the transient temperature and scattering source function distributions. The region starts to cool with the medium at uniform temperature. For this condition, the local emittance around the perimeter was obtained by a numerical solution of the radiative equations, and the rate of heat loss from the entire medium was evaluated. As cooling continues, the emissive ability decreases because of the lower temperatures in the outer regions of the rectangle. Based on some previous work, a lower limit for the transient overall emittance was found by obtaining a similarity solution. For some ranges of optical thickness and scattering albedo, the lower limit is only a small amount below the initial emittance. For these conditions, the initial emittance can be used to compute the entire transient resulting in a considerable simplification.

Nomenclature

A_R = aspect ratio of rectangular region, d/b
a = absorption coefficient of radiating medium, 1/m
B_0 = optical length of small side of rectangle, $(a + \sigma_s)b$
b = length of small side of rectangle, m
c_p = specific heat of radiating medium, KJ/(Kg − K)
d = length of large side of rectangle, m
F = function of X, Y in temperature distribution
G = function of X, Y in $\tilde{T}^{1/4}$
I = source function in absorbing and scattering region, W/(m² − sr); $\tilde{I} = \pi I/\sigma T_i^4$
i = radiation intensity, W/(m² − sr)
K = extinction coefficient, $a + \sigma_s$, 1/m
$L_{e,0}$ = mean beam length for optically thin region, m
Q = heat loss rate from entire perimeter, W
q_r = radiative heat flow per unit area and time, W/m²
R = dimensionless distance between two points
R_1, R_2 = dimensionless distances defined in Eq. (17)
S = distance along a radiation path, m
S_n = function defined in Eq. (9)
T = absolute temperature, K; $\tilde{T} = T/T_i$
T_i = initial temperature or reference temperature, K
x,y,z = rectangular coordinates, m; $X = x/b$, $Y = y/b$, $Z = z/b$
ϵ = emittance
ζ' = intermediate variable in Eq. (8)
ρ = density of radiating medium, Kg/m³
σ = Stefan-Boltzmann constant, W/(m² − K⁴)
σ_s = scattering coefficient, 1/m
τ = time, s; $\tilde{\tau} = (4\sigma T_i^3/\rho c_p b)\tau$
Ω = scattering albedo, $\sigma_s/(a + \sigma_s)$
ω_i = incident solid angle, sr

Subscripts

fd = fully developed transient conditions
m = integrated mean value
o = reference value along boundary

Received Feb. 1, 1989; revision received April 24, 1989.

*Senior Research Scientist, Office of the Chief Scientist, Associate Fellow AIAA.

Introduction

IN Ref. 1, the present author investigated the radiative cooling behavior of a nonscattering two-dimensional rectangular region initially at uniform temperature and then placed into surroundings at a much lower temperature. The medium filling the region was emitting and absorbing, and the governing integrodifferential equation was solved using two-dimensional numerical integration. This type of cooling was shown in Refs. 2 and 3 to have an overall emittance that is bounded by two limits. The emittance is largest when the region is initially at uniform temperature. The emittance decreases during cooling as a result of the more pronounced decrease in the temperature of the outer regions of the rectangle. It was found in Ref. 3 that a constant lower emittance limit is reached because the ratio of the transient heat loss to the fourth power of the mean temperature becomes constant with time. This also applies for a medium with isotropic scattering, which is the subject of the present paper. The cooling behavior of the rectangle depends on its aspect ratio and optical thickness. The solutions in Ref. 1 provided the conditions without scattering for which the two emittance limits are close to each other and, consequently, where the initial emittance can be used as a good approximation throughout an entire transient. When scattering is present, the temperature distributions become more uniform, and this extends the conditions where this approximation is valid. This is investigated here for various values of the scattering albedo.

The solution of the radiation transfer equations in two- and three- dimensional geometries has received increased attention in recent years. Faster computers with greater storage have provided a means for directly evaluating the integral relations or for solving equations that result from applying approximate techniques. Integration with discrete ordinates was used in Refs. 4 to 6. Polynomial approximations for the temperature distributions were used in Refs. 7 and 8, and finite elements were applied in Ref. 9. Additional analyses are in Refs. 10 and 11. These references are typical examples of the studies available in the literature. Most of the previous work has been for steady-state conditions; the effect of transient conditions on local and overall emissive behavior is considered here. The results are of interest for the cooling of high temperature porous ceramic insulators and for elimination of waste heat in outer space by use of particle or liquid drop radiators.

The governing energy and source function equations are solved here by numerical methods using two-dimensional Gaussian integration. This yields transient temperature and

source function distributions. An integration of the effect of these distributions on radiative behavior at the boundary provides local heat losses around the perimeter so that local and overall emittances can be evaluated. The overall emittances are correlated as a function of the optical mean beam length of the rectangular cross section. The correlation reveals the ranges of optical thickness and albedo within which the transient overall emittance does not deviate appreciably from the results for a rectangle at uniform temperature, thus providing a very useful approximation for some ranges of parameters.

Analysis

The geometry is a rectangular region that is long in the z direction (Figs. 1). Conditions are uniform along z so the heat transfer behavior depends only on x,y, and time. The region is a gray absorbing, emitting, and scattering material, and is initially at a uniform temperature T_i that is high compared with the surrounding environment at T_e. The effect of isotropic scattering on transient cooling will be examined by determining the behavior of the radiative energy equations for two limiting conditions. Numerical solutions are used of the appropriate analytical relations.

Radiative Relations for Transient Cooling

The thermal conductivity of the region is assumed small; consequently, the local transient cooling depends on the divergence of the radiative flux (Ref. 12),

$$\rho c_p \frac{\partial T}{\partial \tau} = -\nabla \cdot q_r \tag{1}$$

The local source of radiation depends on local emission and on the scattering of the locally incident intensity. This yields the source function I as

$$I = (1-\Omega)\frac{\sigma T^4}{\pi} + \frac{\Omega}{4\pi}\int_{\omega_i=0}^{4\pi} i\, d\omega_i \tag{2}$$

From Ref. 12 the divergence of the radiative flux has a simple form in terms of the source function I

$$\nabla \cdot q_r = \frac{4a}{\Omega}(\sigma T^4 - \pi I) \tag{3}$$

so that Eq. (1) becomes

$$\rho c_p \frac{\partial T}{\partial \tau} = -\frac{4a}{\Omega}[\sigma T^4(x,y,\tau) - \pi I(x,y,\tau)] \tag{4}$$

The unknowns are T and I, and Eqs. (2) and (4) can be solved simultaneously if i is expressed in terms of these functions. The equation of transfer provides a relation for i along a path starting with $i(0)$ at $S(0)$

$$i(S) = i(0)e^{-KS} + K\int_0^S I(S')e^{-K(S-S')}\, dS' \tag{5}$$

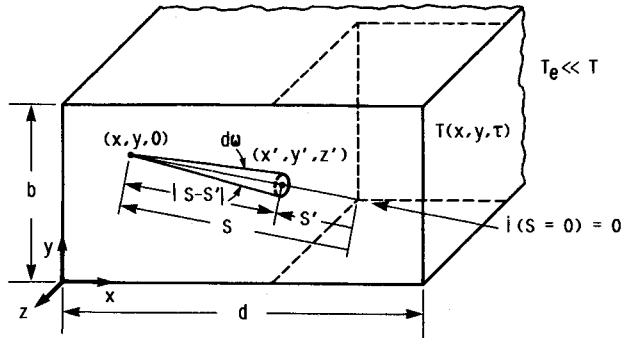

Fig. 1a Emitting absorbing, and scattering medium in two-dimensional rectangular geometry—intensity along path between two interior locations, x',y',z' to $x,y,0$.

Since the surrounding temperature is low, the $i(0) \approx 0$, and Eq. (5) is substituted into Eq. (2) to yield

$$I = (1-\Omega)\frac{\sigma T^4}{\pi} + \frac{\Omega}{4\pi}K\int_{\omega_i=0}^{4\pi}\int_{S'=0}^{S} I(S')\frac{e^{-K(S-S')}}{(S-S')^2}(S-S')^2\, d\omega_i dS' \tag{6}$$

The $(S-S')^2\, d\omega_i$ is the cross section of a volume element at $S-S'$, and dS' is its length; hence $(S-S')^2 d\omega_i dS' = dV$. Then in rectangular coordinates at any time τ,

$$I(x,y) = (1-\Omega)\frac{\sigma T^4(x,y)}{\pi} + \frac{\Omega}{2\pi}K\int_{x'=0}^{d}\int_{y'=0}^{b}\int_{z'=0}^{\infty} I(x',y')\frac{e^{-K[(x-x')^2+(y-y')^2+z'^2]^{1/2}}}{(x-x')^2+(y-y')^2+z'^2}\, dx'dy'dz' \tag{7}$$

The z integration is carried out by letting $\zeta' = [(x-x')^2 + (y-y')^2]^{1/2}$ and $t = [1+(z'/\zeta')^2]^{1/2}$. Equation (7) then takes the form

$$I(x,y) = \frac{a}{K}\frac{\sigma T^4(x,y)}{\pi} + \frac{\sigma_s}{4}\int_{x'=0}^{d}\int_{y'=0}^{b}\frac{I(x',y')}{\zeta'}S_1(K\zeta')\, dx'dy' \tag{8}$$

The S_1 is one of the functions S_n examined in Ref. 13

$$S_n(x) = \frac{2}{\pi}\int_1^\infty \frac{e^{-xt}}{t^n(t^2-1)^{1/2}}dt = \frac{2}{\pi}\int_0^{\pi/2} e^{-x/\cos\theta}\cos^{n-1}\theta d\theta \tag{9}$$

Eqs. (4) and (8) are placed in dimensionless form to yield

$$\frac{\partial \tilde{T}}{\partial \tilde{\tau}} = B_0\frac{1-\Omega}{\Omega}[\tilde{I}(x,y,\tau) - \tilde{T}^4(x,y,\tau)] \tag{10}$$

$$\tilde{I}(X,Y,\tilde{\tau}) = (1-\Omega)\tilde{T}^4(X,Y,\tilde{\tau}) + \frac{\Omega B_0}{4}\int_{X'=0}^{A_R}\int_{Y'=0}^{1}\tilde{I}(X,Y,\tilde{\tau})\frac{S_1(B_0R)}{R(X,Y,X',Y')}dX'dY' \tag{11}$$

where $R(X,Y,X',Y') = [(X-X')^2 + (Y-Y')^2]^{1/2}$.

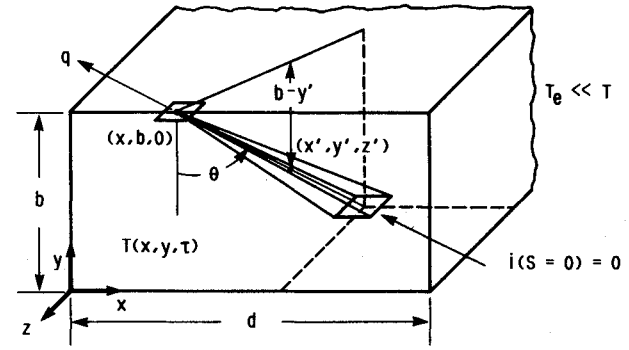

Fig. 1b Intensity along path between interior and surface locations, x',y',z' to $x,b,0$.

Surface Heat Fluxes

After a solution is found for $\bar{T}$ and $\bar{I}$ from Eqs. (10) and (11), the local energy fluxes leaving the boundary of the rectangular region are obtained. Referring to Fig. 1b, the q_y that passes out of the region through the element at $(x,b,0)$ arises from all the volume elements in the region. From the form of Eq. (5), an element with path length dS' at S' contributes an intensity $KI(S')e^{-K(S-S')}$ at S. The contribution to q_y is $i\cos\theta\, d\omega$. Using $\cos\theta = (b-y')/(S-S')$ and $dV = (S-S')^2 d\omega\, dS'$, the contribution to q from dV is $KI(S')e^{-K(S-S')}[(b-y')/(S-S')^3]\, dV$. Then by integrating over all volume elements

$$q_y = 2K\int_{x'=0}^{d}\int_{y'=0}^{b}\int_{z'=0}^{\infty} I(x',y') \times (b-y')\frac{e^{-K[(x-x')^2+(b-y')^2+z'^2]^{1/2}}}{[(x-x')^2+(b-y')^2+z'^2]^{3/2}}\,dx'dy'dz' \quad (12)$$

Letting $\xi_2 = [(x-x')^2+(b-y')^2]^{1/2}$, this is transformed to the form

$$q(x,b) = \pi K\int_{x'=0}^{d}\int_{y'=0}^{b} I(x',y')\frac{b-y'}{\xi_2^2(x,x',y')}S_2(K\xi_2)\,dx'dy' \quad (13a)$$

Similarly the local flux leaving the right side of the rectangle is

$$q(d,y) = \pi K\int_{x'=0}^{d}\int_{y'=0}^{b} I(x',y')\frac{d-x'}{\xi_1^2(y,x',y')}S_2(K\xi_1)\,dx'dy' \quad (13b)$$

where $\xi_1 = [(d-x')^2+(y-y')^2]^{1/2}$

Emittance Relations

The overall emittance for the entire rectangle was obtained in two ways to check the numerical calculations. From an overall heat balance, the mean temperature would be known; therefore this is the characteristic temperature on which the emittance is based. The overall heat balance gives $2(b+d)\epsilon\sigma T_m^4 = -\rho c_p bd\, dT_m(\tau)/d\tau$, which has the dimensionless form

$$\epsilon(\tilde{\tau}) = -\frac{2A_R}{1+A_R}\frac{1}{\bar{T}_m^4}\frac{d\bar{T}_m}{d\tilde{\tau}} \quad (14)$$

where

$$\bar{T}_m(\tilde{\tau}) = \frac{1}{A_R}\int_{X=0}^{A_R}\int_{Y=0}^{1}\ddot{T}(X,Y,\tilde{\tau})\,dXdY \quad (15)$$

Then by use of Eq. (10)

$$\epsilon(\tilde{\tau}) = -\frac{2}{1+A_R}\frac{B_0}{\bar{T}_m^4}\frac{1-\Omega}{\Omega}\int_{X=0}^{A_R}\int_{Y=0}^{1} \ddot{I}(X,Y,\tilde{\tau}) - \ddot{T}^4(X,Y,\tilde{\tau})]dXdY \quad (16)$$

The local emittance along the boundary of the rectangle can be found from the surface heat fluxes in Eq. (13),

$$\epsilon(X,1) = \frac{q(x,b)}{\sigma T_m^4} = \frac{B_0}{\bar{T}_m^4}\int_{X'=0}^{A_R}\int_{Y'=0}^{1} \ddot{I}(X',Y')\frac{1-Y'}{R_1^2}S_2(B_0R_1)dX'dY' \quad (17a)$$

$$\epsilon(A_R,Y) = \frac{q(d,y)}{\sigma T_m^4} = \frac{B_0}{\bar{T}_m^4}\int_{X'=0}^{A_R}\int_{Y'=0}^{1} \ddot{I}(X',Y')\frac{A_R-X'}{R_2^2}S_2(B_0R_2)dX'dY' \quad (17b)$$

where $R_1^2 = (X'-X)^2+(Y'-1)^2$ and $R_2^2 = (X'-A_R)^2+(Y'-Y)^2$.

The energy emitted around the entire boundary divided by $2(b+d)\sigma T_m^4$ than gives the emittance for the rectangle as

$$\epsilon = \frac{1}{1+A_R}\left[\int_{X=0}^{A_R}\epsilon(X,l)dX + \int_{Y=0}^{1}\epsilon(A_R,Y)dY\right] \quad (18)$$

Two solutions will now be obtained for which the overall emittances are bounds for the transient cooling process.

Solution for Region at Uniform Temperature

First, consider very short times. Since the region is initially at uniform temperature, the early emittance behavior is for $T(x,y,\tau) = T_i$ and $T_m = T_i$. Letting $\ddot{T} = 1$ in Eq. (11), the source function $\ddot{I}(X,Y,)$ is found from the integral equation.

$$\ddot{I}(X,Y) = 1-\Omega+\Omega\frac{B_0}{4}\int_{X'=0}^{A_R}\int_{Y'=0}^{1} \ddot{I}(X',Y')\frac{S_1(B_0R)}{R(X,Y,X',Y')}dX'dY' \quad (19)$$

The ϵ values ($\epsilon \equiv \epsilon_{ut}$) are then found from Eqs. (16) to (18) using $\ddot{T} = \ddot{T}_m = 1$.

Solution for Fully Developed Transient Cooling

After the rectangular region has partially cooled (about 30%, as shown by previous work for other region shapes), a separation of variables solution becomes valid where the overall heat loss at any time becomes proportional to the T_m^4 at that time. The overall ϵ becomes constant with time; this is $\epsilon \equiv \epsilon_{fd}$, and it is smaller than ϵ_{ut} because of the relatively cool outer regions of the rectangle. To obtain this transient solution, let T and $I^{1/4}$ have the forms,

$$\ddot{T}(X,Y,\tilde{\tau}) = \ddot{T}_0(X_0,Y_0,\tilde{\tau})F(X,Y) \quad (20a)$$

$$\ddot{I}^{1/4}(X,Y,\tilde{\tau}) = \ddot{T}_0(X_0,Y_0,\tilde{\tau})G(X,Y) \quad (20b)$$

where x_0, Y_0 is an arbitrary location. Substituting into Eq. (10), the spatial at time variables become separated,

$$\frac{1}{\bar{T}_0^4}\frac{d\ddot{T}_0}{d\tilde{\tau}} = B_0\frac{1-\Omega}{\Omega}\frac{G^4-F^4}{F} \quad (21)$$

This shows that the quantity $(G^4-F^4)/F$ must be constant. The $F(A_R/2,0)$ is arbitrarily set equal to unity so that from the right side of Eq. (21).

$$G^4(X,Y) - F^4(X,Y) = F(X,Y)[G^4(A_R/2,0) - 1] \quad (22a)$$

When Eq. (20) is substituted into Eq. (11), the result is

$$G^4(X,Y) = (1-\Omega)F^4(X,Y) + \Omega\frac{B_0}{4}\int_{X'=0}^{A_R}\int_{Y'=0}^{1} G^4(X',Y')\frac{S_1(B_0R)}{R(X,Y,X',Y')}dX'dY' \quad (22b)$$

Equations (22a) and (22b) are solved simultaneously by a numerical procedure as will be described. From Eqs. (15) and (20a), $\bar{T}_m = T_oF_m$ where F_m is from the same definition as Eq. (15). Then from Eq. (16)

$$\epsilon_{fd} = -\frac{2B_0}{1+A_R}\frac{1-\Omega}{\Omega}\frac{1}{F_m^4}\int_{X=0}^{A_R}\int_{Y=0}^{1}(G^4-F^4)dXdY$$

Equation (22a) is then substituted into the integral and by use of the definition for F_m, the ϵ_{fd} becomes

$$\epsilon_{fd} = 2B_0\frac{1-\Omega}{\Omega}\frac{A_R}{1+A_R}\frac{1}{F_m^3}[1-G^4(A_R/2,0)] \quad (23)$$

This is not a function of time and depends on the parameters B_0, Ω, and A_R. The second way of computing ϵ_{fd} is from Eq. (18). By use of Eq. (20), the relations in Eq. (17) become

$$\epsilon_{fd}(X,1) = \frac{q(x,b)}{\sigma T_m^4} = \frac{B_0}{F_m^4}\int_{X'=0}^{A_R}\int_{Y'=0}^{1} G^4(X',Y')\frac{1-Y'}{R_1^2}S_2(B_0R_1)dX'dY' \tag{24a}$$

$$\epsilon_{fd}(A_R,Y) = \frac{q(d,y)}{\sigma T_m^4} = \frac{B_0}{F_m^4}\int_{X'=0}^{A_R}\int_{Y'=0}^{1} G^4(X',Y')\frac{A_R-X'}{R_2^2}S_2(B_0R_2)dX'dY' \tag{24b}$$

Optically Thin Conditions

For an optically thin region, $B_0 << 1$, and Eq. (22b) becomes $G^4(X,Y) = (1-\Omega)F^4(X,Y)$. Since $F(A_R/2,0) = 1$, $G^4(A_R/2,0) = 1-\Omega$ and Eq. (23) becomes (note that $F_m \to 1$ for small B_0 as verified by Table 1),

$$\epsilon_{fd} = 2B_0(1-\Omega)\frac{A_R}{1+A_R} = 2ab\frac{A_R}{1+A_R}$$

The mean beam length for an optically thin region (Ref. 12) is $L_{e,o} = 4V/A = 2bd/(b+d) = 2bA_R/(1+A_R)$. Hence for an optically thin region,

$$\epsilon_{fd} = aL_{e,o} = (1-\Omega)(a+\sigma_s)L_{e,o} \tag{25}$$

which is independent of the scattering coefficient. From Eqs. (11) and (16), the same result is found, that, for the uniform temperature case, $\epsilon_{ut} \to \alpha L_{e,o}$ for small B_o.

Numerical Solution

To obtain results for the fully developed transient condition, Eqs. (22a) and (22b) are solved numerically for $F(X,Y)$ and $G(X,Y)$. To begin the iterative procedure, $F(X,Y) = 1$ was substituted into Eq. (22b), which was then solved for $G^4(X,Y)$ by an inner iteration loop. To increase the convergence rate, an acceleration factor of 1.5 was used after each iteration. The new $G^4(X,Y)$ was substituted into Eq. (22a), which was solved for $F(X,Y)$ by Newton's method. This was substituted into (22b) to continue the main iteration process until the relative changes in F^4 and G^4 at all X,Y were less than 10^{-4}. Some results were checked for accuracy by lowering this limit to 10^{-5}. Typical running times were 30 min on an IBM 370 computer. For the medium at uniform temperature, the solution was obtained much more rapidly, since only Eq. (19) was solved. This is the same as Eq. (22b) with $F(X,Y) = 1$ and hence is the converged result at the end of the first iteration of the previous solution.

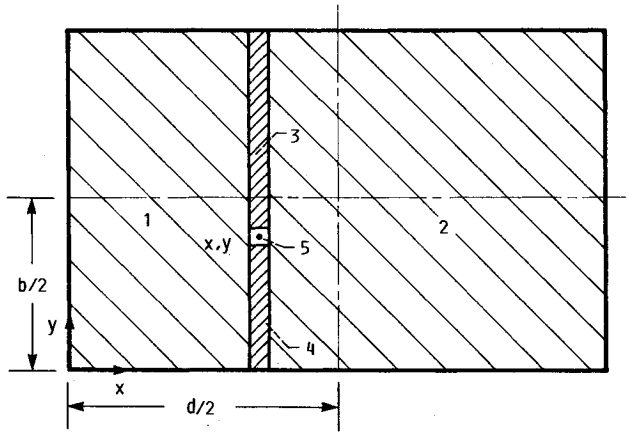

Fig. 2 Two-dimensional regions for integrating radiative transfer relations.

As described in more detail in Ref. 1 for the $\Omega = 0$ case, the double integration in Eq. (22b) was carried out by using two-dimensional Gaussian integration. The rectangle was covered with a square grid; 30 increments were usually used across the short side. Two-dimensional spline fits were made of $G^4(X,Y)$ [or $\tilde{I}(X,Y)$ in Eq. (19)] and values of the function were interpolated between the grid points as required by the integration routine. The number of integration points in each coordinate

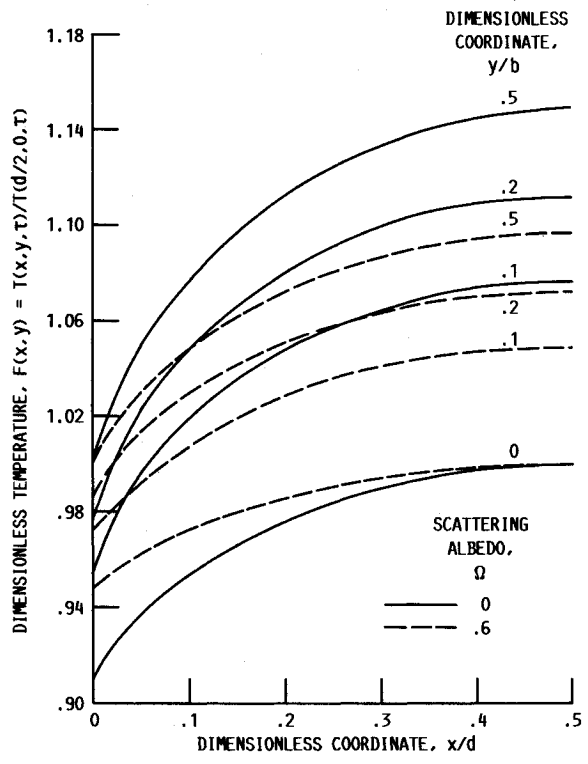

Fig. 3a Temperature distributions for fully developed cooling of a square region ($d/b = 1$)—optical dimension, $B_0 = (a+\sigma_s)b = 2$.

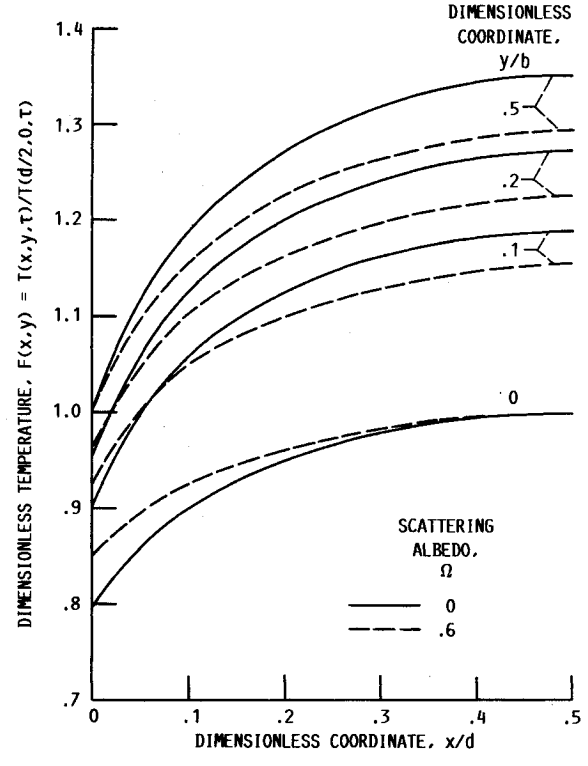

Fig. 3b Optical dimension, $B_0 = (a+\sigma_s)b = 6$.

Table 1 Overall emittance values for cooling of a rectangular region at uniform temperature and for fully developed transient conditions

(a) Aspect ratio, $d/b = 1$

Optical dimension, $(a + \sigma_s)b$	Emittance, mean F	Scattering albedo, Ω 0	0.3	0.6	0.9
1	ϵ_{ut}	0.570	0.457	0.306	0.0926
	ϵ_{fd}	0.565	0.455	0.305	0.0926
	F_m	1.041	1.032	1.022	1.007
2	ϵ_{ut}	0.767	0.653	0.479	0.170
	ϵ_{fd}	0.739	0.638	0.474	0.169
	F_m	1.076	1.065	1.049	1.018
4	ϵ_{ut}	0.887	0.794	0.634	0.282
	ϵ_{fd}	0.776	0.717	0.601	0.280
	F_m	1.135	1.124	1.103	1.048
6	ϵ_{ut}	0.926	0.838	0.692	0.348
	ϵ_{fd}	0.711	0.685	0.606	0.341
	F_m	1.187	1.174	1.155	1.084

(b) Aspect ratios, $d/b = 2,4$

Optical dimension, $(a + \sigma_s)b$	Emittance, mean F	Aspect ratio 2		4	
		Scattering albedo, Ω 0	0.6	0	0.6
1	ϵ_{ut}	0.656	0.375	0.708	0.422
	ϵ_{fd}	0.646	0.373	0.695	0.420
	F_m	1.040	1.024	1.040	1.026
2	ϵ_{ut}	0.832	0.553	0.874	0.605
	ϵ_{fd}	0.783	0.543	0.818	0.590
	F_m	1.075	1.053	1.081	1.061
4	ϵ_{ut}	0.925	0.687	0.951	0.726
	ϵ_{fd}	0.757	0.626	0.774	0.657
	F_m	1.140	1.115	1.156	1.133

direction was usually about six times the number of grid points. The numerical difficulty for small R in the denominator of Eq. (22b) was avoided by using cylindrical coordinates for a small region around the point X, Y (area 5 in Fig. 2) so that $dX'dY'/R$ becomes $dRd\Theta$. From symmetry, integrations were carried out around grid points in only one quadrant. The rectangle was divided into five integration areas, as shown in Fig. 2. Similar procedures were used to evaluate ϵ_{fd} and ϵ_{ut} from Eqs. (24), (16), and (17). Four integration areas were used because the thin vertical strip in Fig. 2 is then along the boundary (see Ref. 1 for more information).

Results and Discussion

Temperature Distributions

The overall emittance is bounded by two values for the transient cooling studied here. The highest value is when the rectangle is initially at uniform temperature. The lower limit is reached during the transient when the normalized profile shapes for the temperature and source function become independent of time. These shapes are found from the simultaneous solution of Eqs. (22a) and (22b). The temperature at the center of the long side is used as a convenient reference value, and the distribution $F(x,y) = T(x,y,\tau)/T(d/2,0,\tau)$ is shown for some sample cases in Figs. 3. If it is desired to obtain temperatures relative to the instantaneous mean temperature, then $T(x,y,\tau)/T_m(\tau) = F(x,y)/F_m$ where F_m is in Table 1. The temperature profiles in this "fully developed" transient cooling region depend on the scattering albedo, the aspect ratio, and a characteristic optical dimension $B_0 = (a + \sigma_s)b$.

The results in Figs. 3 are for a square region; half of each symmetric profile is shown. Figure 3a is for thickness $B_0 = 2$, and results with scattering, $\Omega = 0.6$, are compared with those for a medium that is only emitting and absorbing, $\Omega = 0$. Since energy is flowing outward from within the medium, the temperatures decrease continuously from the center toward the

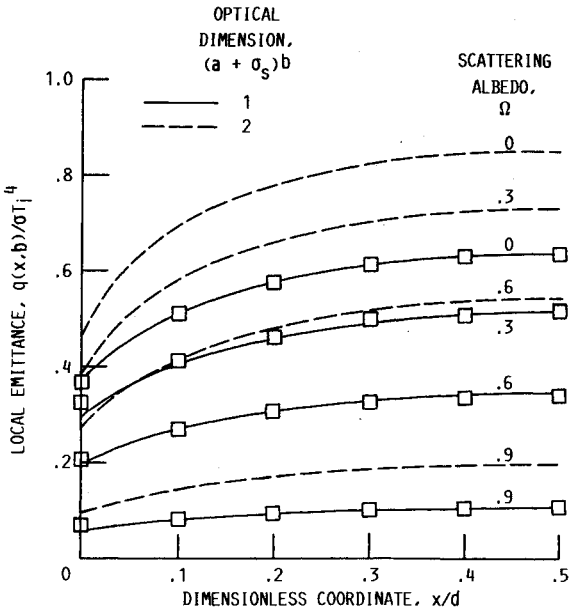

Fig. 4a Local emittance around boundary for square region at uniform temperature ($d/b = 1$; square points are from Kim and Lee.[6] —optical dimension, $B_0 = (a + \sigma_s)b = 1$ and 2.

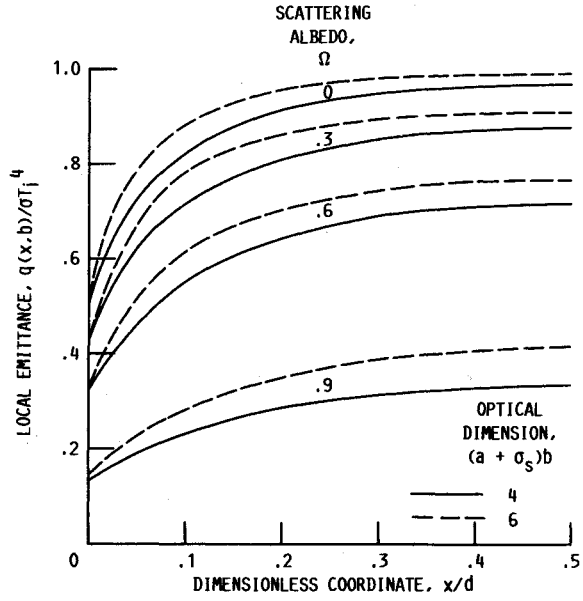

Fig. 4b Optical dimension, $B_0 = (a + \sigma_s)b = 4$ and 6.

boundaries with the lowest temperature at the corners. The profiles are rather flat for this optical thickness. Scattering results in a redistribution of energy within the medium and for $\Omega = 0.6$, the temperature amplitudes are approximately one-half those without scattering. In Fig. 3b, the optical thickness is increased to 6; the temperature profiles are similar to those in Fig. 3a but have about twice the amplitude. Scattering is not as effective in redistributing energy for this larger temperature variation.

Boundary Heat Fluxes

After the temperature and source function distributions have been calculated, the local emitted heat flux can be obtained along the boundaries of the rectangle. For the region at uniform temperature, T_i, Eq. (17) is used with $\bar{I}(X,Y)$ from Eq. (19), and results for local emittance along the boundary of a square are in Fig. 4. From symmetry, only one-eighth of the perimeter is shown, and results are given for four B_0 and Ω. For

the medium at uniform temperature, the emittance increases with optical thickness and approaches blackbody emission at the center of the side when $B_0 = 6$. Local emission near the corners is about one-half that at the center of the sides. For all optical thicknesses, the emittance decreases significantly as Ω is increased. Overall emittance values obtained by integrating around the boundary. Eq. (18), are given in Table 1. The results show how the heat radiated away from the entire rectangle increases with optical thickness and decreases with scattering albedo. There are numerical results in Ref. 6 for radiation from an isothermal square with $B_0 = 1$. Figure 11 of that reference is for $\Omega = 0$, 0.1, 0.5, and 0.9. Results were directly compared with the present solutions for $\Omega = 0$ and 0.9, and values were interpolated for $\Omega = 0.3$ and 0.6. An enlargement was made of the figure in Ref. 6 so that accurate values could be obtained. Excellent agreement was obtained with the present results.

Figures 5 show the local heat loss behavior for fully developed transient cooling of a medium with a square cross sec-

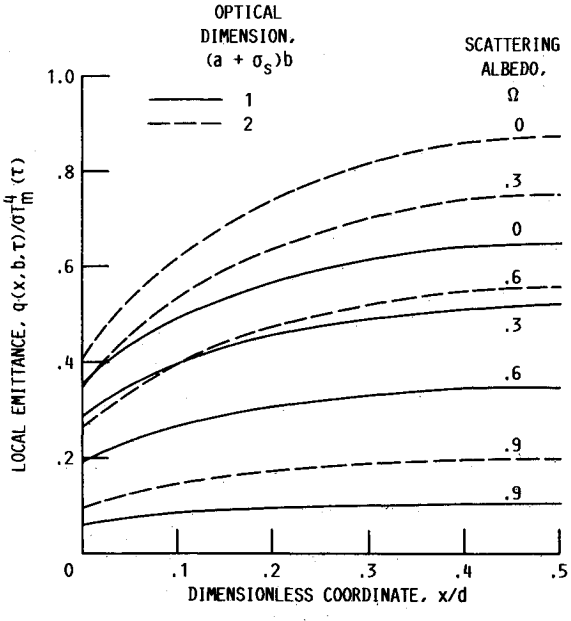

Fig. 5a Local emittance [based on $T_m^4(\tau)$] around boundary for square region during fully developed transient cooling—optical dimension, $B_0 = (a + \sigma_s)b = 1$ and 2.

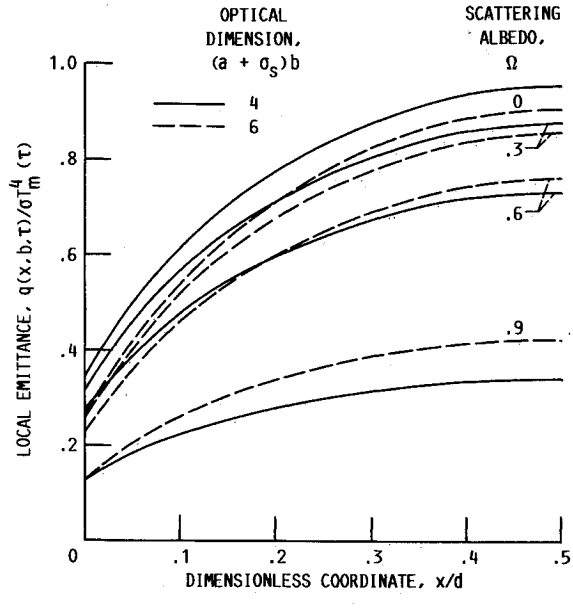

Fig. 5b Optical dimension, $B_0 = (a + \sigma_s)b = 4$ and 6.

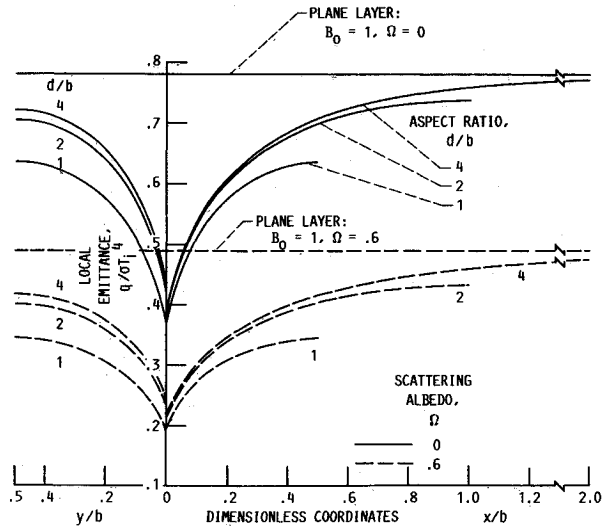

Fig. 6a Local emittance along boundary for radiating rectangular region at uniform temperature—optical dimension, $B_0 = (a + \sigma_s)b = 1$.

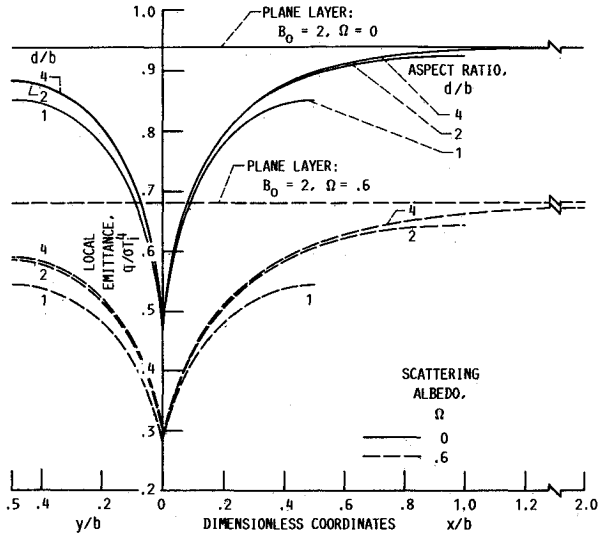

Fig. 6b Optical dimension, $B_0 = (a + \sigma_s)b = 2$.

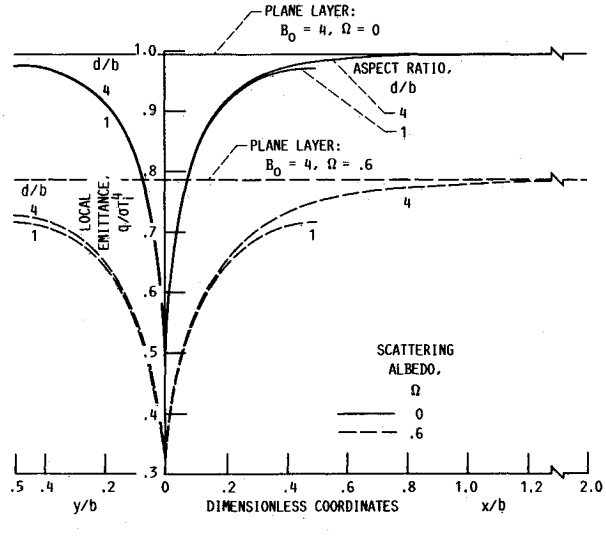

Fig. 6c Optical dimension, $B_0 = (a + \sigma_s)b = 4$.

tion. For this cooling condition, the local $q(\tau)$ is normalized by dividing by $\sigma T_m^4(\tau)$; the resulting ratio is independent of time in the fully developed regime. For $B_0 = 1$ and 2, the results in Fig. 5a are very similar to those in Fig. 4a. This is due to the fact that for small optical thicknesses, and especially in conjunction with large Ω, the temperature distribution tends to be rather uniform, and hence the fully developed transient results are close to those for uniform temperature. For larger $B_0 = 4$ and 6, Fig. 5b differs significantly from Fig. 4b. For a large optical thickness, the outer regions of the medium become quite cool relative to the interior; this results in a decrease in the local emittance as B_0 is increased. The result is that some of the curves for $B_0 = 6$ are now below those for $B_0 = 4$.

In Figs. 6 and 7, results are given for additional aspect ratios, $d/b = 2$ and 4. Figures 6 is for the local emittance $q/\sigma T_i^4$ around the boundary for the entire region at uniform temperature T_i, and Figs. 7 show $q(\tau)/\sigma T_m^4(\tau)$ during fully developed transient cooling. The three parts of each figure are for $B_0 = 1$, 2, and 4, and results are given for $\Omega = 0$ and 0.6. The values are also shown for a plane layer from Refs. 2 and 3. In Figs. 6, as the rectangle becomes elongated, the local emittance along the central portion of the long side approaches that for a plane layer. The approach is more rapid as the optical thickness is increased as this tends to isolate the influence of the cooler end regions. The center of the long side has close to plane layer behavior for $B_0 = 1$ when $d/b \approx 4$, but for $B_0 = 4$, only $d/b \approx 1$ is required if $\Omega = 0$ and $d/b \approx 2$ if $\Omega = 0.6$.

Turning now to Fig. 7 for fully developed transient cooling, the local emittances are independent of time because the local $q(\tau)$ and $T_m^4(\tau)$ both decrease at the same rate. The $T_m(\tau)$ was chosen as a characteristic temperature as it would be available from the cooling history. If desired, the values of $F_m = T_m(\tau)/T(d/2,0,\tau)$ in Table 1 can be used to renormalize the local ϵ on the basis of a characteristic surface temperature. Unless the region is optically thin, the local heat loss depends primarily on the adjacent local temperatures, which can exceed or be less than T_m. For example, at the center of the long side, the surface temperature could exceed the mean temperature, which has been decreased by the cooler end regions. This can cause the local emittance, which is based on T_m^4, to be greater than unity. This does not imply that local emission exceeds that of a blackbody. The values larger than unity arise because the mean temperature of the medium can differ considerably from the temperatures governing local emission. As the aspect ratio increases, the ϵ along the long side will eventually become equal to the ϵ_{fd} for a plane layer as the end regions contribute less significantly to the average behavior. This is shown by the curves for $d/b = 2$ and 4 on the right side of Fig. 7c.

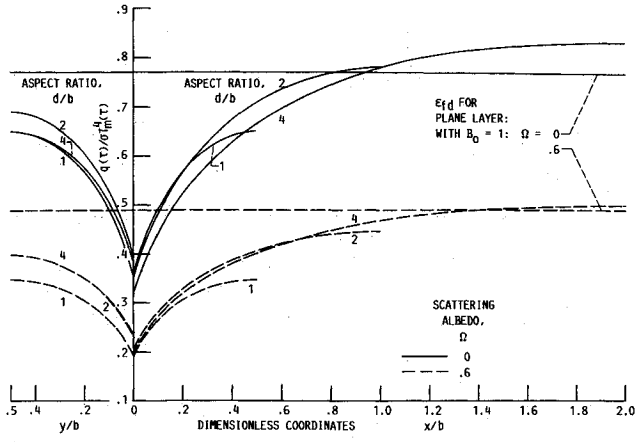

Fig. 7a Local emittance [based on $T_m^4(\tau)$] along boundary for fully developed transient cooling—optical dimension, $B_0 = (a + \sigma_s)b = 1$.

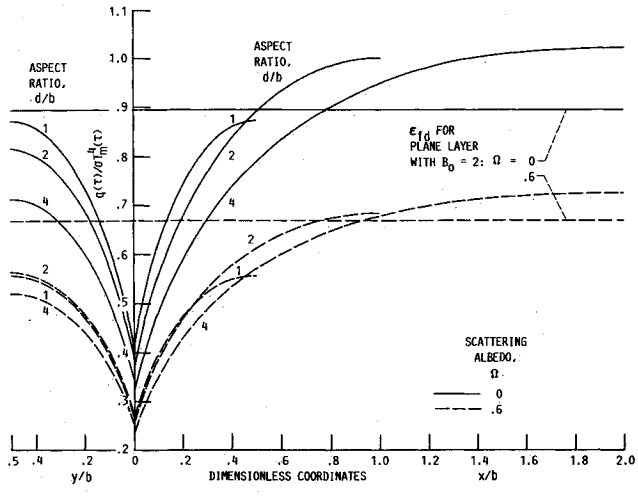

Fig. 7b Optical dimension, $B_0 = (a + \sigma_s)b = 2$.

Overall Emittance Values

Figures 8 and 9 show overall emittance values such that, for the upper and lower emittance bounds, the instantaneous heat losses from the entire rectangle are $Q_{ut} = 2(b + d)\epsilon_{ut}\sigma T_i^4$ and $Q_{fd} = 2(b + d)\epsilon_{fd}\sigma T_m^4$. For a square geometry, Fig. 8a gives ϵ_{ut} and ϵ_{fd} as a function of B_0. For each Ω, the $\epsilon_{fd} \approx \epsilon_{ut}$ for B_0 below a value that increases with Ω. For larger B, the ϵ_{fd} is below ϵ_{ut} as a result of the cooling of the outer regions of the rectangle which decreases its emissive ability. This is especially true for small Ω and large B_0, the conditions that produce larger temperature gradients. The characteristic length $L_{e,0}$ in Fig. 8 is the mean beam length for an optically thin rectangle as defined in connection with Eq. (25). This is a useful dimension for comparing results for various aspect ratios in Fig. 8b as it causes the curves for each Ω to fall along one line for small abscissas. As shown by Eq. (25), the abscissa could be multiplied by $1 - \Omega$ to bring all the curves together for small $L_{e,0}$. This would cause the dashed lines in Fig. 8b to move to the left to coincide with the solid lines for small abscissas. Figure 8b shows where ϵ_{fd} falls below ϵ_{ut} for various aspect ratios and for $\Omega = 0$ and 0.6. The differences between the two ϵ begin at about $(a + \sigma_s)L_{e,0} = 1.5$ for $\Omega = 0$, and at 2 for $\Omega = 0.6$. Below these $(a + \sigma_s)L_{e,0}$ the ϵ_{ut} can be used throughout the entire transient cooling process. The ϵ_{fd} decreases substantially below ϵ_{ut} as $(a + \sigma_s)L_{e,0}$ becomes larger.

The variation of the overall emittance values with aspect ratio is shown in Fig. 9. At the right end of the abscissa scale are the values for a plane layer (infinite aspect ratio). When

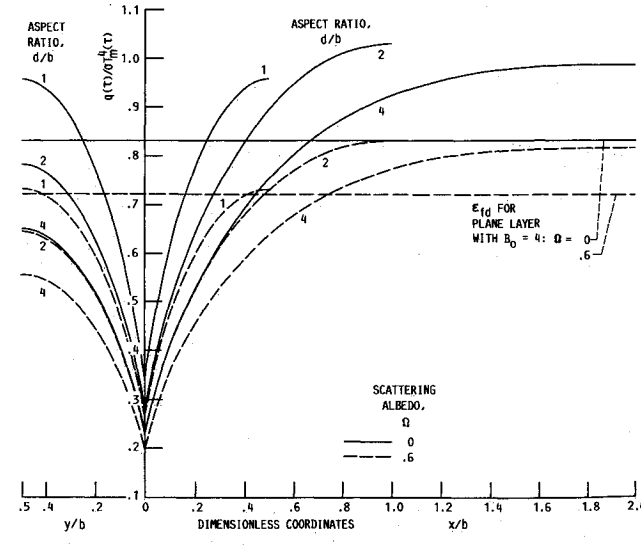

Fig. 7c Optical dimension, $B_0 = (a + \sigma_s)b = 4$.

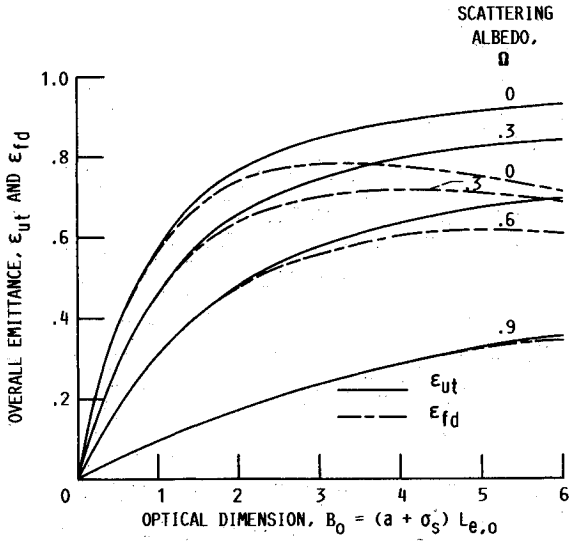

Fig. 8a Emittance bounds for transient cooling of a rectangular region initially at uniform temperature—square geometry ($L_{e,0} = b$).

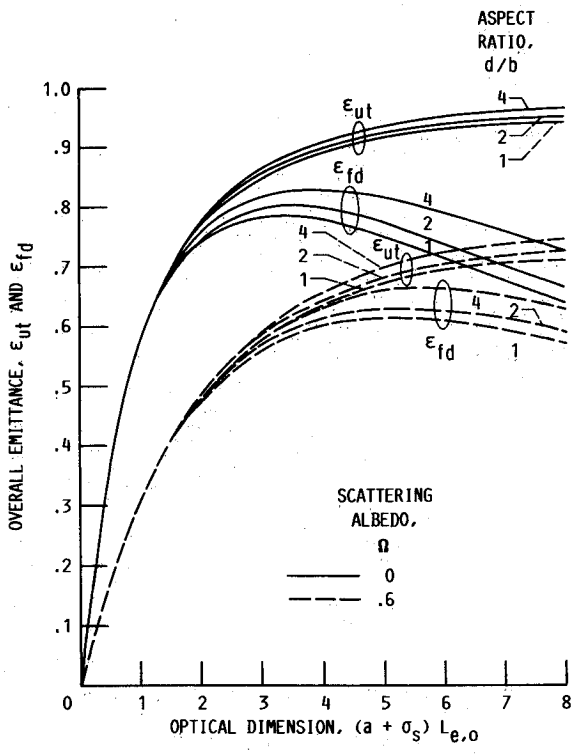

Fig. 8b Aspect ratios, 1, 2, and 4.

$d/b < 1$, the geometry as drawn on the figure, becomes a thin vertical rectangle with a thickness that decreases toward zero as d/b decreases. The rectangle then begins to act as an optically thin region. Plane layer results are gradually approached as d/b increases, and the effect of the cooler end regions on the average behavior is thereby decreased.

Conclusions

The equations for the temperature and scattering source function were solved numerically for two limiting conditions during transient radiative cooling of a rectangular medium that emits, absorbs, and scatters isotropically. The local and overall heat fluxes leaving the boundary of the medium were then obtained. The situation studied was for cooling in an environment at a much lower temperature than the temperatures in the region. For transient cooling starting with the region initially at uniform temperature, previous analyses for plane layers and cylinders showed that a similarity behavior developed after the region had lost about 30% of its energy. The transient energy loss becomes proportional to the fourth power of the mean temperature, and the cooling is characterized by a constant emittance that is a function of aspect ratio, optical thickness, and scattering albedo. The time when this solution occurs can be estimated by using the transient cooling equation [Eq. (14)] until a 30% energy loss is obtained when using a constant overall emittance value between the isothermal and fully developed values.

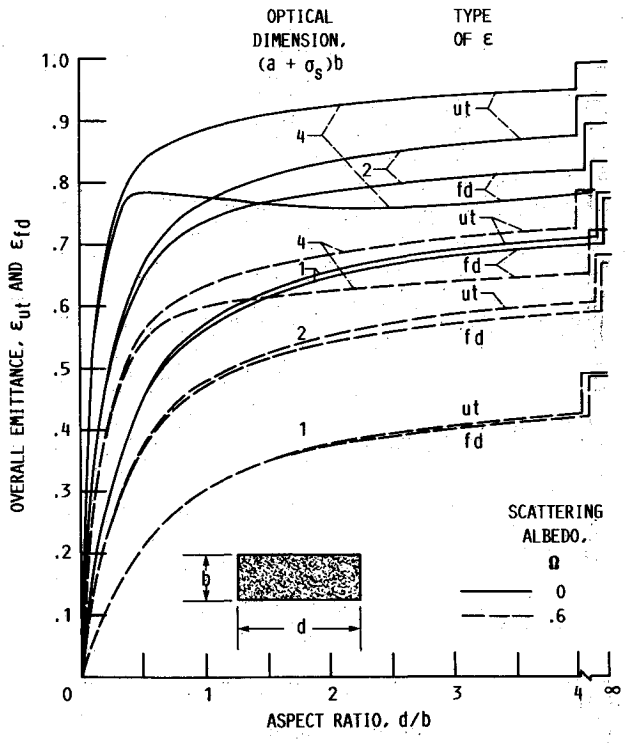

Fig. 9 Emittance bounds of rectangular region as a function of aspect ratio.

The details of the local emittance variation around the perimeter of the region depend on the parameters, but as would be expected, the lowest values are always at the corners, and the highest are at the center of the long side. For the region at uniform temperature and no scattering, the heat flux near the corners is about one-half the maximum value. When $\Omega = 0.6$, the value of the flux at the corner may be somewhat more depressed relative to the maximum. For the fully developed transient cooling condition, the corner regions decrease further in temperature, and the local heat flux variation around the boundary becomes more accentuated.

The overall emittances that govern the heat loss from the entire perimeter were presented as a function of the optical mean beam length. Scattering significantly reduces the emittance values. A comparison of the emittance upper and lower bounds, ϵ_{ut} and ϵ_{fd}, shows that, for any aspect ratio, the ϵ_{ut} can be used within about 3% accuracy throughout the entire cooling process if $(a + \sigma_s)L_{e,0}$ is less than about 1.75 for $\Omega = 0$ and less than 2.5 for $\Omega = 0.6$. For larger $(a + \sigma_s)L_{e,0}$, the ϵ_{fd} begins to drop below ϵ_{ut}

Acknowledgment

The assistance is gratefully acknowledged of Mr. Frank Molls of the National Aeronautics and Space Administration, Lewis Research Center. He provided considerable help in developing the computer program to solve the radiative integral equations.

References

[1]Siegel, R., "Some Aspects of Transient Cooling of a Radiating Rectangular Medium," *International Journal of Heat and Mass Transfer* (to be published).

[2]Siegel, R., "Transient Radiative Cooling of a Droplet-Filled Layer," *Journal of Heat Transfer,* Vol. 109, No. 1, Feb. 1987, pp. 159–164.

[3]Siegel, R., "Separation of Variables Solution for Non-Linear Radiative Cooling," *International Journal of Heat and Mass Transfer,* Vol. 30, No. 5, May 1987, pp. 959–965.

[4]Fiveland, W. A., "Discrete-Ordinates Solutions of the Radiative Transport Equation for Rectangular Enclosures," *Journal of Heat Transfer,* Vol. 106, No. 4, Nov. 1984, pp. 699–706.

[5]Fiveland, W. A., "Three-Dimensional Radiative Heat-Transfer Solutions by the Discrete-Ordinates Method," *Journal of Thermophysics and Heat Transfer,* Vol. 2, No. 4, Oct. 1988, pp. 309–316.

[6]Kim, T.-K. and Lee, H., "Effect of Anisotropic Scattering on Radiative Heat Transfer in Two-Dimensional Rectangular Enclosures," *International Journal of Heat and Mass Transfer,* Vol. 31, No. 8, Aug. 1988, pp. 1711–1721.

[7]Yuen, W. W. and Wong, L. W., "Analysis of Radiative Equilibrium in a Rectangular Enclosure With Gray Medium," *Journal of Heat Transfer,* Vol. 106, No. 2, May 1984, pp. 433–440.

[8]Yuen, W. W. and Ho. C. F., "Analysis of Two-Dimensional Radiative Heat Transfer in a Gray Medium With Internal Heat Generation," *International Journal of Heat and Mass Transfer,* Vol. 28, Jan. 1985, pp. 17–23.

[9]Razzaque, M. M., Howell, J. R., and Klein, D. E., "Coupled Radiative and Conductive Heat Transfer in a Two-Dimensional Rectangular Enclosure With Gray Participating Media Using Finite Elements," *Journal of Heat Transfer,* Vol. 106, No. 3, Aug. 1984, pp. 613–619.

[10]Crosbie, A. L. and Schrenker, R. G., "Radiative Transfer in a Two-Dimensional Rectangular Medium Exposed to Diffuse Radiation," *Journal of Quantitative Spectroscopy and Radiative Transfer,* Vol. 31, No. 4, 1984, pp. 339–372.

[11]Ho, C. H. and Ozisik, M. N., "Combined Conduction and Radiation in a Two-Dimensional Rectangular Enclosure," *Numerical Heat Transfer,* Vol. 13, No. 2, 1988, pp. 229–239.

[12]Siegel, R. and Howell, J. R., *Thermal Radiation Heat Transfer,* 2nd ed., Hemisphere, Wash., D.C., 1981, Chap. 14.

[13]Yuen, W. W. and Wong, L. W., "Numerical Computation of an Important Integral Function in Two-Dimensional Radiative Transfer," *Journal of Quantitative Spectroscopy and Radiative Transfer,* Vol. 29, No. 2, 1983, pp. 145–149.